

Enhanced visible light absorption and reduced charge recombination in AgNP plasmonic photoelectrochemical cell



Samaila Buda^{a,*}, Suhaidi Shafie^{a,b}, Suraya Abdul Rashid^{a,c}, Haslina Jaafar^b, N.F.M. Sharif^b

^a Institute of Advanced Technology, Universiti Putra Malaysia, 43400 UPM Serdang, Selangor Darul Ehsan, Malaysia

^b Department of Electrical and Electronics Engineering, Faculty of Engineering, Universiti Putra Malaysia, 43400 UPM Serdang, Selangor Darul Ehsan, Malaysia

^c Department of Chemical Engineering, Faculty of Engineering, Universiti Putra Malaysia, 43400 UPM Serdang, Selangor Darul Ehsan, Malaysia

ARTICLE INFO

Article history:

Received 12 June 2017

Received in revised form 30 June 2017

Accepted 4 July 2017

Available online 8 July 2017

Keywords:

Nanoparticle

Silver

Plasmonic

Power

Photon

ABSTRACT

In this research work, silver nanoparticles (AgNP) were synthesized using a simple solvothermal technique, the obtained AgNP were used to prepare a titania/silver (TiO₂/Ag) nanocomposites with varied amount of Ag contents and used to fabricated a photoanode of dye-sensitized solar cell (DSSC). X-ray photoelectron spectroscopy (XPS) was used to ascertain the presence of silver in the nanocomposite. A photoluminance (PL) spectra of the nanocomposite powder shows a low PL activity which indicates a reduced electron-hole recombination within the material. UV-vis spectra reveal that the Ag in the DSSC photoanode enhances the light absorption of the solar cell device within the visible range between $\lambda = 382$ nm and 558 nm nm owing to its surface plasmon resonance effect. Power conversion efficiency was enhanced from 4.40% for the pure TiO₂ photoanode based device to 6.56% for the device fabricated with TiO₂/Ag due to the improvement of light harvesting caused by the localized surface plasmonic resonance effect of AgNP. The improvement of power conversion was also achieved due to the reduced charge recombination within the photoanode.

© 2017 Universiti Putra Malaysia, UPM. Published by Elsevier B.V. This is an open access article under the CC BY-NC-ND license (<http://creativecommons.org/licenses/by-nc-nd/4.0/>).

Introduction

Solar energy is the world's most abundant and clean energy source which make it the most viable alternative to the exhaustible environmentally harmful fossil fuels. Dye-sensitized solar cell (DSSC) has received a great attention over other types of solar cells because of its low production cost, ease of production and low toxicity [1]. Considerable efforts have been focused over the last two decades for the improvement of the solar cell efficiency since it was first invented by Gratzel and co-workers in 1991, such efforts include development of new sensitizers [2], electrolyte development [3], contact optimization [4], counter electrodes [5], and semiconductor photoanode [6].

The overall efficiency of DSSC depends largely on the semiconductor photoanode because of its role in dye uptake, charge collection and carrier transport [7]. Semiconductors such as ZnO and SnO₂ were used as photoanode materials in DSSC. Among the various semiconductor materials, Titanium dioxide (TiO₂) is the most viable candidate for use in DSSC because of its superior qualities of large surface area for maximum dye loading and suitable band-gap [8]. However, TiO₂ nanoparticle-based photoanode has a ran-

dom electron transport paths which hinders cell performance due to high electron-hole recombination along this paths [9].

There is a growing body of literature that recognize the importance of modification of TiO₂-based photoanode for improved efficiency of DSSC such as by replacing the nanoparticles with one dimensional nanotubes and nanowires [10] and modification of metal nanoparticles [11]. Recently, Ag nanoparticles were incorporated into the TiO₂ nanoparticles for improved efficiency of DSSC [12]. The surface plasmon resonance properties of Ag nanoparticles plays an important role in improving the efficiency of dye-sensitized solar cell through the enhancement of light absorption properties of the photoanode of the DSSC [13]. Similarly AgNP reduce electron-hole recombination within the photoanode, thus improving the charge transfer process in the photoanode.

Protection of the bare Ag particles against corrosion by electrolyte and also to control its sizes and distribution on the TiO₂ surface is essential for optimum utilization of the plasmonic DSSC [9,14]. Till now, few methods of Ag/TiO₂ nanocomposite preparation were employed which include (i) chemical reduction method [15] and (ii) photoreduction method [16,17]. However, the drawbacks of these methods are the stability of the unprotected AgNP against the corrosive electrolyte and difficulty in controlling the size of the NP which is an important parameter that determining the surface plasmon effect of the nanoparticles.

* Corresponding author.

E-mail address: budasamaila@gmail.com (S. Buda).

In this study, we developed a simple method to prepare a protected and size controlled Ag nanoparticles uniformly distributed on the TiO₂ surface by solvothermal process for application in DSSC).

Experimental methods

Materials

Titanium dioxide (TiO₂), Fluorine Tin Oxide (FTO) coated glass (7Ωsq⁻¹), Di-2 cis-bis (isothiocyanato) bis-bipyridyl-4-4-dicarboxylato ruthenium (II) (N719) dye were obtained from Sigma- Aldrich Co., (USA). Silver nitrate was purchased from Qrec chemicals, and liquid electrolyte was obtained from Solaronix (Switzerland). X-ray photoelectron spectroscopy was performed using a PHI II Quantera (ULVAC-PHI, Inc.), Electrochemical impedance spectroscopy (EIS) was carried out using Autolab PGSTAT204, current- voltage characteristics of the DSSC device were obtained using Keithly Source Meter (Keithly 2611,USA) under AM 1.5 light intensity.

Synthesis of Ag

AgNPs were synthesized using solvothermal method as follows. 1 g of polyvinylpyrrolidone (PVP) was dissolved in 30 ml ethylene glycol at room temperature, and to this solution, 50mg of AgNO₃ dissolved in 20 ml ethylene glycol was added. The mixture was then stirred continuously until complete dissolution of the silver nitrate particles was achieved, the solution was then transferred into an agitated reactor with a sealed Teflon autoclave and put in an oven maintaining a temperature of 120 °C for 12 hrs and then allow to cool to room temperature. The resulting solution was washed by centrifugation at 1000 rpm for 5 s using water and ethanol to remove EG and PVP. Finally, the resultant Ag NPs was protected by coating with TiO₂ solution obtained by mixing 10 mL of titanium (iv) isopropoxide in acetyl acetone in molar ratio of 1:1

Preparation of DSSC photoanode and device assembly

TiO₂/Ag paste was prepared using commercial TiO₂ nanoparticles powder without any purification. Firstly, 500mg of TiO₂ and a varied amount of Ag NP (1, 2.5, 5, 7.5 and 10, wt%) was mixed with 0.2 ml of acetic acid, 0.4 ml DI water, 2.5 ml absolute ethanol and 1.6 g of α-terpineol and vigorously stirred for 1hr followed by sonication for 30 min for obtaining solution A. Also, 0.25 g of ethyl cellulose in 2.5 ml ethanol were mixed using a magnetic stirrer for 1 h for obtaining solution B. Then Solutions A and B were homogeneously mixed with magnetic stirrer for 12 h and the resultant solution was evaporated until 10% of the original volume was obtained. The paste was coated on an FTO glass by screen printing method. The photoanode was sensitized by immersing in Di-tetrabutylammonium cis-bis(2,2'-bipyridyl-4,4'-dicarboxylato) ruthenium(II) (N719) dye solution in 1:1 acetonitrile/*tert*-butyl alcohol for up to 18hrs to ensure optimum dye loading and then rinsed in ethanol to remove un-adsorbed dye. For the counter electrode fabrication, A 0.01 M of H₂PtC₁₆ (in ethanol) was spin coated over an FTO glass electrode which was then dry in air followed by heating on a hot plate at 400 °C for 20 min. The photoanode and platinum counter electrode were then sealed together with a transparent film of Surlyn 1472 (Dupont) cut as a frame around the photoanode film. An acetonitrile-based electrolyte containing 0.05 M iodine, 0.1 M lithium iodide, 0.5 M 4-*tert*-butylpyridine (TBP), and 0.7 M tetrabutylammonium iodide (TBAI) was introduced through the holes pre-drilled on the counter electrode, which were sealed immediately with glue as shown in Fig. 1

Results

X-ray photoelectron analysis

To verify the presence of silver nanoparticles in the TiO₂/Ag composite synthesized by solvothermal method, the X-ray photoelectron spectroscopy of the prepared TiO₂/Ag power were recorded. The narrow scan for the silver particle is shown in Fig. 2. Two peaks for AgNP located at 367.72 eV and 373.72 eV of

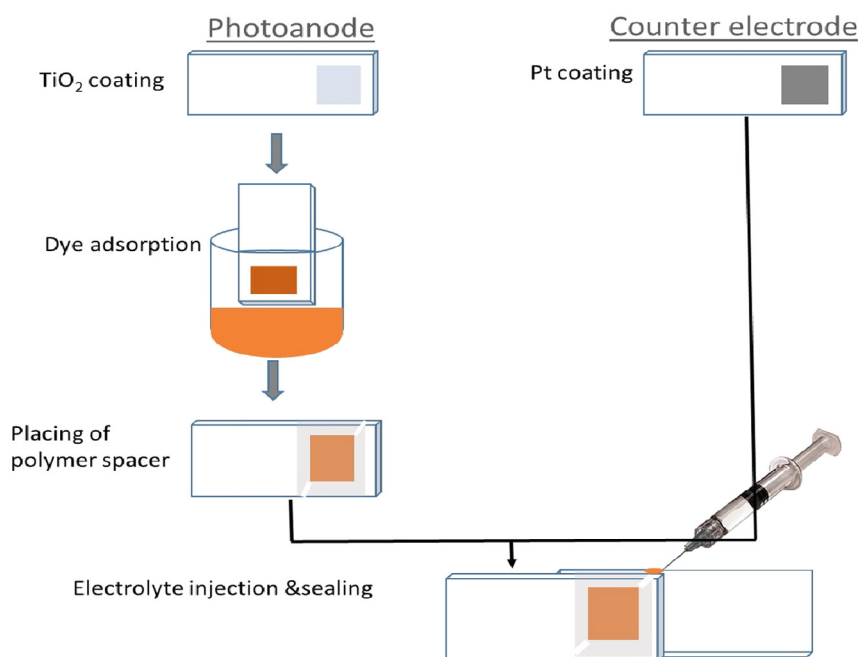


Fig. 1. Pictorial presentation of DSSC device assembly.

the TiO₂/Ag composite are seen from the plot. The peak at 373.73 eV is attributed to a bonding states of Ag₂O while the second peak seen at 367.6 eV is a characteristic chemical bonding state of Ag⁰ in the Ag 3d5/2 XPS peaks [18,19].

Optical properties of the TiO₂/AgNP composite

To determine the light absorption of the TiO₂/Ag composite, UV–visible absorption data for bare TiO₂ and TiO₂/Ag were measured as shown in Fig. 3. No visible light absorption was seen on the bare TiO₂, the surface plasmon resonance effect of Ag in the TiO₂/Ag composite influenced the visible light absorption in the range between 400 nm and 550 nm with a peak at 460 nm which marched with the absorption peak of N719 dye [20], this demonstrate a proper design for the plasmonic DSSC [21]. The absorption edge for TiO₂/Ag has also been shifted toward the red end of the visible region which will enhance the overall light absorption of the solar cell.

In order to evaluate the influence of Ag concentration on the optical properties of the TiO₂/Ag composite, Samples prepared with 1 wt%, 2.5 wt%, 5 wt%, 7.5 wt%, and 10 wt% of AgNP were evaluated. The optical absorption as a function of wavelength is plotted as shown in Fig. 4.

All the samples prepared with AgNP content have shown a significant improvement in light absorption within the visible range between 382 nm and 558 nm, the intensity of the light absorbance varied with the Ag concentration, it is clear from the plot that the light absorption rises proportionally with the increase in the plasmonic metal concentration. In contrast with the TiO₂/Ag samples, the pure TiO₂ sample did not show any visible light absorption. It is evident that the incorporation of plasmonic silver metal

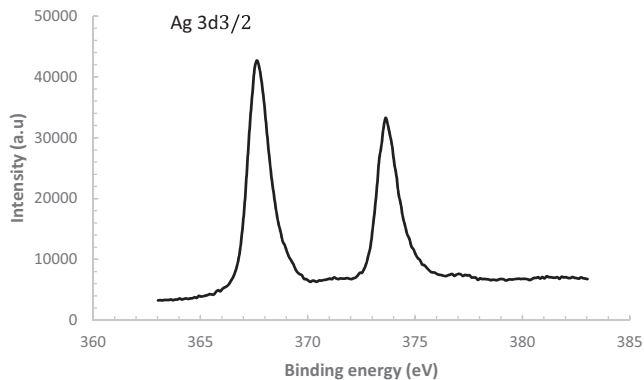


Fig. 2. Binding energy of silver nanoparticle in the TiO₂/Ag composite.

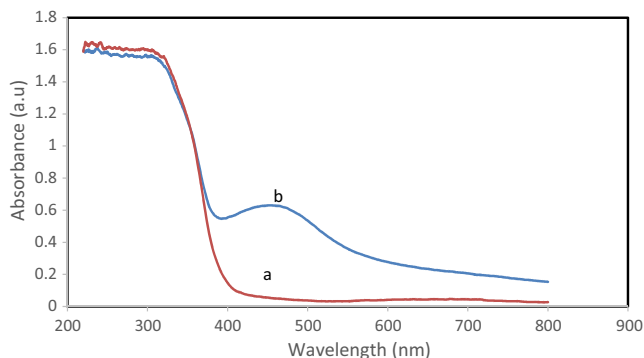


Fig. 3. Absorption spectra for (a) TiO₂ and (b) TiO₂/Ag composite.

nanoparticle can greatly influence the optical properties of TiO₂ particles.

Electron-hole recombination in the Pure TiO₂ and TiO₂/Ag based photoanode were analysed using a well-known technique of photoluminescence spectroscopy. Knowledge of charge transport dynamics of a photoanode material is important since it is used for the design of suitable plasmonic material type and concentration for improvement of the photovoltaic performance of a plasmonic DSSC.

Incident photons with energy equal to or higher than the band-gap energy of semiconductor material produces photoinduced charge carriers and the recombination of these carries is attended with the release energy in the form of photoluminescence in proportion to the amount of these charges that recombined. Therefore, an observed lower PL intensity for a material indicates less charge recombination.

Fig. 5 shows a photoluminescence spectra of the pure and TiO₂/Ag composite. The pure TiO₂ has shown a high PL intensity between 360 nm and 550 nm indicating a high charge recombination within the semiconductor, conversely, upon addition of AgNP, the PL intensity was seen to have been suppressed. A Schottky barrier was created at the Ag–TiO₂ interface which could serve as an electron sink which, in effect reduces the electron-hole recombination within the TiO₂ semiconductor material [22,23].

Photovoltaic properties of TiO₂/Ag-based DSSC

The current–voltage behaviour of the DSSCs were appraised under simulated solar radiation of AM 1.5. The achieved photocur-

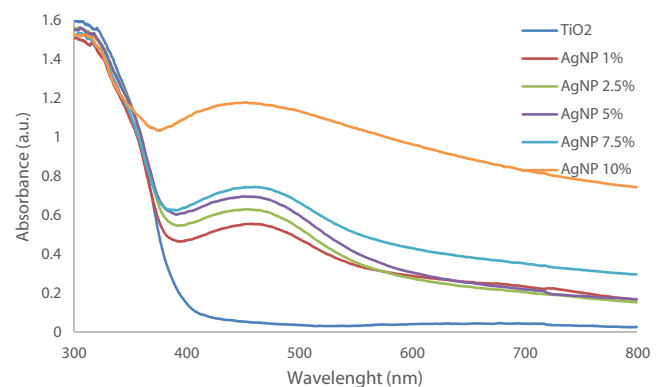


Fig. 4. Absorption spectra of TiO₂/Ag synthesized with different Ag concentration.

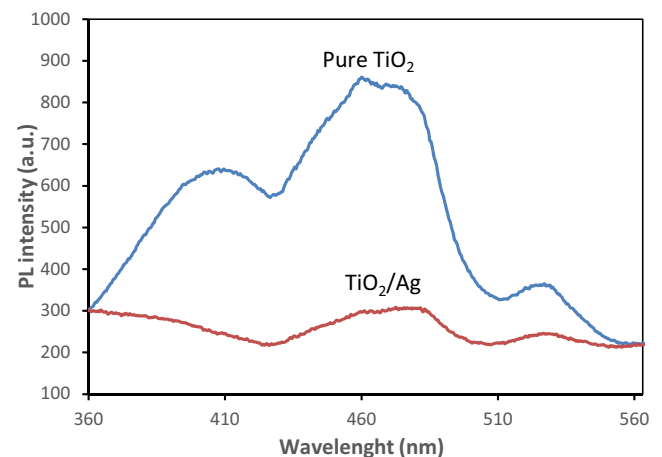


Fig. 5. Photoluminescence spectra of modified and unmodified titania powder.

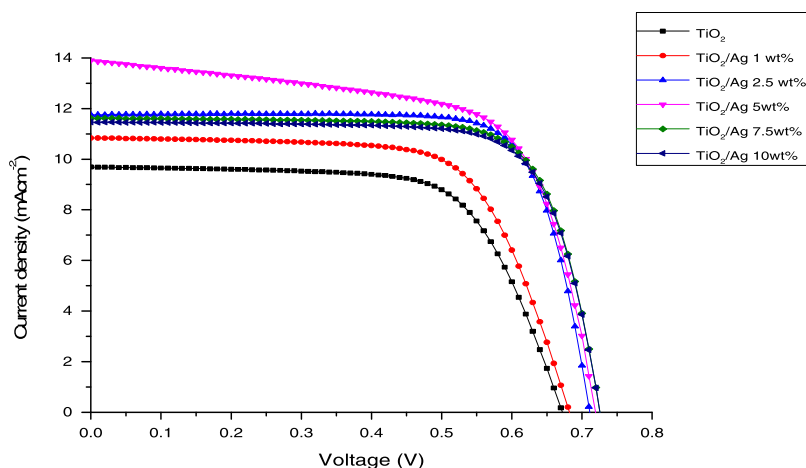


Fig. 6. Current density–voltage characteristics of TiO₂/Ag solar cells under standard illumination conditions (AM1.5).

Table 1

Current density–voltage characteristics of DSSC device fabricated with pure TiO₂ and TiO₂/AgNP.

Photoanode	J _{sc} (mAcm ⁻²)	V _{oc} (V)	J _{max} (mAcm ⁻²)	V _{max} (V)	FF	η (%)
TiO ₂	9.69	0.69	8.79	0.5	0.66	4.40
TiO ₂ /Ag1	10.83	0.69	9.65	0.52	0.67	5.02
TiO ₂ /Ag2.5	11.76	0.71	11	0.58	0.76	6.38
TiO ₂ /Ag5	13.86	0.72	11.5	0.57	0.66	6.56
TiO ₂ /Ag7.5	11.59	0.73	10.7	0.59	0.75	6.31
TiO ₂ /Ag10	11.34	0.73	10.5	0.59	0.75	6.20

rent density–voltage (J–V) curves are shown in Fig. 6, and the deduced photovoltaic parameters are enumerated in Table 1.

The pure TiO₂ photoanode based DSSC recorded a current density of 9.69 A cm⁻², open circuit voltage of 0.69 V and a power conversion efficiency of 4.40%, upon addition of AgNP, the TiO₂/Ag (1 wt% of Ag) plasmonic DSSC showed an increase in the current density to 10.83 A cm⁻² leading to a higher power conversion efficiency 5.02% representing a percentage increase of 14.09% over the pure TiO₂ based device. The improved photovoltaic performance is achieved due to the plasmonic effect of Silver and fast interfacial charge transfer from the Ag nanoparticles on the TiO₂ [24].

Optimization of Ag content on TiO₂ is necessary for high-performance of the DSSC as well as minimizing the production cost. It is shown from Table 1 that Ag concentration from 1 wt% up to 5 wt% resulted in the linear rise in both the photocurrent density from 10.83 A cm⁻² to 13.86 A cm⁻² as well increase of open circuit voltage from 0.69 V to 0.72 V respectively. Further addition of Ag on the TiO₂ surface beyond 5 wt% revealed a decrease in the J_{sc} to 11.59 A cm⁻² at 7.5 wt% and further down to 11.34 A cm⁻² for the photoanode containing 10 wt%. The observed results noticeably revealed that the conversion efficiency of a DSSC was enhanced with an increase in the Ag content of the photoanode till it reached its maximum at 5 wt%, afterwards, a further increase in the Ag content led to the drop in conversion efficiency.

In contrast to the J_{sc}, the V_{oc} has consistently risen with increase in Ag content from 1 wt% until 10 wt% this is because of the effect of silver particle on the TiO₂ which rises its Fermi level which in effect rises the open circuit voltage which is known to be the difference between the Fermi level of the semiconductor and the redox potential of the electrolyte of the DSSC [25].

The drop in the power conversion efficiency at high Ag concentration (7.5 wt% and 10 wt%) might be due to the free standing AgNP on the titania structure which may oxidized and then cor-

roded by the liquid electrolyte thereby becoming a recombination centre, where the photogenerated charge carrier injected into the TiO₂ are annihilated causing the decrease in the J_{sc} [26].

Another drawback of the excess of silver concentration is that the free standing AgNP occupy more site in the TiO₂ crystal resulting in reduction of the active surface area on the TiO₂ surface which should be available for more dye uptake that will lead to more electron–hole generation in the DSSC [27].

Charge transfer in Ag/TiO₂ photoanode based DSSC

The overall DSSC device performance can be directly measured by measuring its I–V characteristics behaviour in which the open circuit voltage, short circuit current and fill factor can be deduced from the measurement. But no detailed information about the dynamics of charge transfers leading to the behaviour of the cell as well as resistances of specific sub-components of the device that influences the device performance can be obtained from the measurement.

To understand the interfacial charge transfer inside the fabricated DSSC, electrochemical impedance spectroscopy (EIS) measurements was carried out in a frequency range between 0.01 Hz and 100 kHz, and presented in Fig. 7. It shows a plot of semicircles in the middle-frequency for the TiO₂ and TiO₂/Ag photoanode based DSSCs. The intersection a semicircle at the x-axis represents the total series resistance of the device (R_s) while the length of the arc of the semi-circle between 1 and 1000 Hz denotes the charge transfer resistance (R_{ct}) between the photoanode and the electrolyte interface [26,23].

It can be seen from Fig. 7 that the R_s values for pure TiO₂ is 31.43Ω and that of TiO₂/Ag 1 wt% is measured at 28.21Ω, this represent a 10.2% decrease in device resistance as the bare TiO₂ is fortified with just 1 wt% of AgNP. Additionally, the R_{ct} increases

Table 2
Charge transfer parameters of the fabricated DSSCs.

Photoanode	R_s (Ω)	R_{ct} (Ω)	F_{max}	C_μ (μF)	τ_s (ms)	τ_n (ms)	η_c (%)
TiO ₂	31.43	9.61	3146	5.26	0.17	0.05	23.42
TiO ₂ /Ag 1	28.21	11.21	2479	4.99	0.14	0.06	28.44
TiO ₂ /Ag 2	20.18	21.27	2315	4.92	0.10	0.07	51.31
TiO ₂ /Ag 3	16.73	20.59	1018	5.46	0.09	0.16	55.17
TiO ₂ /Ag 4	24.05	13.93	1484	4.32	0.10	0.11	36.68
TiO ₂ /Ag 5	27.44	12.68	1887	5.28	0.14	0.08	31.61

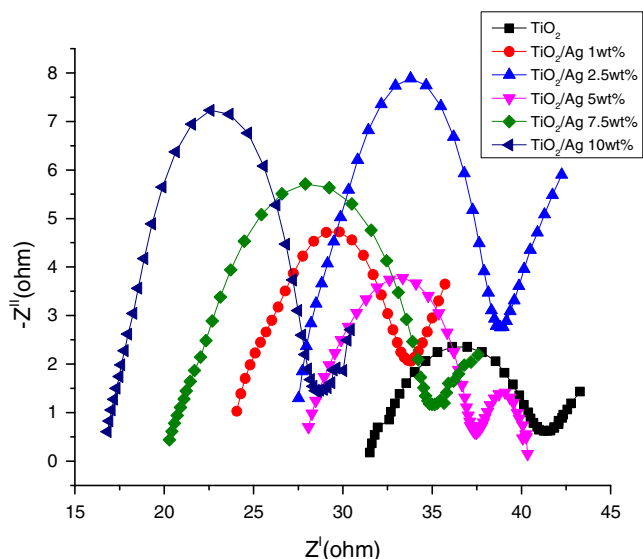


Fig. 7. Nyquist plot of EIS data for the Fabricated DSSCs.

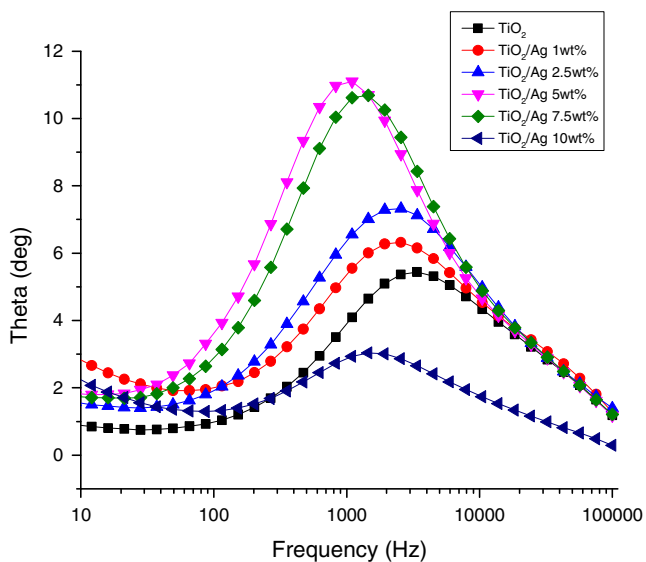


Fig. 8. Bode phase plot of EIS data for the Fabricated DSSCs.

by 10.2% from the 9.61 Ω for pure TiO₂ to a higher value of 11.21 Ω for TiO₂/Ag1wt%. This increase in the R_{ct} value could enhance the J_{sc} as well as the open-circuit voltage (V_{oc}) device.

Table 2 present the summary of the charge transfer process parameters obtained from the EIS measurement as deduced from the Nyquist and Bode phase plots in Figs. 7 and 8 respectively. The table shows a gradual decrease in the R_s value from 28.21 Ω

down to 16.73 Ω as the AgNP content is increase from 1 wt% to 5 wt% while further increase of AgNPs to 7.5 wt% and 10 wt% resulted in the increase in the R_s to a high value of 27.44 Ω indicating that the AgNP content has reached its maximum at 5 wt%. Similarly, the R_{ct} rises from 11.21 Ω at 1 wt% until it reaches its maximum with 5 wt% of AgNP concentration and thereafter declined by further addition of AgNP.

The Bode phase plot of the pure TiO₂ and the titania with varied amount of AgNP is the plot of phase angle against the frequency. It is observed from this plot, that the maximum frequency (F_{max}) has shifted from 3146 Hz to a lower frequency of 2846 Hz with the addition of 1 wt% of AgNP, this trend continued as a function of AgNP content until the concentration reaches 5 wt% where a significant rise in F_{max} was recorded.

Lower value of F_{max} means high electron life time, $\tau_n = 1/(2\pi f)$ [28,29], this high electron life time is caused by a minimal charge recombination process in the DSSC thereby increasing the charge collection efficiency, $\eta_c = (1 + R_s/R_{ct})$ [30], thus electrons with longer τ_n values will subsist the recombination. The increase of electron lifetime causes the back reaction between the electrons within TiO₂ surface and electrolyte to be weak resulting in high current density.

The decrease of τ_n for AgNP content more than 5 wt% is as a result of the excess Ag being oxidized and consequently acting as a recombination sites in the TiO₂ surface.

Conclusion

We have synthesized AgNPs using a simple solvothermal process, the incorporation of the silver nanoparticle in the photoanode of the DSSC has significantly increases the photon absorption of the solar cell, the ability of the AgNP to act as an electron sink within the photoanode has to a larger extent reduced the rapid electron-hole recombination within the TiO₂ thereby enhancing the charge collection efficiency from 23.42% to as high as 55.17%. The improvement of light absorption in the visible light region by the influence of the localized surface plasmon effect of the AgNP has boosted the charge generation of the TiO₂/Ag photoanode based DSSC.

Acknowledgement

This research work was fully sponsored by a Universiti Putra Malaysia grant (PUTRA IPB/2016/9515402).

References

- [1] O'Regan B, Grätzel M. A low-cost, high-efficiency solar cell based on dye-sensitized colloidal TiO₂ films. *Nature* 1991;353:737–40.
- [2] Parisi ML, Maranghi S, Basosi R. The evolution of the dye sensitized solar cells from Grätzel prototype to up-scaled solar applications: a life cycle assessment approach. *Renew Sustain Energy Rev* 2014;39:124–38.
- [3] Snaith L, Schmidt-Mende HJ. Advances in liquid-electrolyte and solid-state dye-sensitized solar cells. *Adv Mater* 2007;19:3187–200.
- [4] Pelet M, Moser S, Grätzel J-E. Cooperative effect of adsorbed cations and iodide on the interception of back electron transfer in the dye sensitization of nanocrystalline TiO₂. *J Phys Chem B* 2000;104:1791–5.

- [5] Nair SV, Sara Thomas AS, Deepak TG, Anjusree GS, Arun TA. A review on counter electrode materials in dye-sensitized solar cells. *Mater Chem A* 2013;207890.
- [6] Hongsith K, Hongsith N, Wongratanaphisan D, Gardchareon A, Phadungditidhada S, Choopun S, Efficiency Enhancement of ZnO Dye-sensitized Solar Cells by Modifying Photoelectrode and Counterelectrode, vol. 79;2015.
- [7] Narayanan R, Burda MAE-SC, Chen X. Chemistry and properties of nanocrystals of different shapes. *Chem Rev* 2005;105:1025–102.
- [8] Xu H, Tao X, Wang D-T, Zheng Y-Z, Chen J-F. Enhanced efficiency in dye-sensitized solar cells based on TiO₂ nanocrystal/nanotube double-layered films. *Electrochim Acta* 2010;55(7):2280–5.
- [9] S. P. Lim, Y. S. Lim, A. Pandikumar, H. N. Lim, Y. H. Ng, R. Ramaraj, D. C. S. Bien, O. K. Abou-Zied, and N. M. Huang, "Gold-silver@TiO₂ nanocomposite-modified plasmonic photoanodes for higher efficiency dye-sensitized solar cells," *Phys. Chem. Chem. Phys.*, vol. 353, no. i, pp. 737–740, 2017.
- [10] C. P. and E. K. Jongbeom Na, Jeonghun Kim, TiO₂ nanoparticulate-wire hybrids for highly efficient solid-state dye-sensitized solar cells using SSP-PEDOTs, *Rsc Adv*, 4(84), 44555–44562; 2014.
- [11] B. L. and C. L. X. Zhang, Y. Zhu, X. Yang, S. Wang, J. Shen, "SiO₂-Ag-SiO₂-TiO₂ multi-shell structures: plasmon enhanced photocatalysts with wide-spectral-response," *Nanoscale*, vol. 5, pp. 3359–3366, 2013.
- [12] Samaila B, Shafie S, Rashid SA, Jaafar H, Khalifa A. Response surface modeling of photogenerated charge collection of silver-based plasmonic dye-sensitized solar cell using central composite design experiments. *Results Phys*. 2017;7:493–7.
- [13] D. A. S. and J. J. Mock, M. Barbic, D. R. Smith and S. Schultz, No TitleShape effects in plasmon resonance of individual colloidal silver nanoparticles, *J Chem Phys*, 116, 6755–6759; 2002.
- [14] Mandal P, Sharma S. Progress in plasmonic solar cell efficiency improvement: a status review. *Renew Sustain Energy Rev* 2016;65:537–52.
- [15] Lau WM, Binyu Yu JY, Leung Kar Man, Guo Qiuquan. Synthesis of Ag–TiO₂ composite nano thin film for antimicrobial application. *Nanotechnology* 2011;22(11):115603.
- [16] Photiphitak C, Rakkwamsuk P, Muthitamongkol P, Sae-Kung C, Thanachayanont C. Effect of silver nanoparticle size on efficiency enhancement of dye-sensitized solar cells. *Int J Photoenergy* 2011;2011:1–8.
- [17] Shao Feng Chen WXH, Li Jian Ping, Qian Kun, Xu Wei Ping, Lu Yang, Hong ASHY. Large scale photochemical synthesis of M@TiO₂ nanocomposites (M = Ag, Pd, Au, Pt) and their optical properties, CO oxidation performance, and antibacterial effect. *Nano Res* 2010;3(4):244–55.
- [18] Bomben KD, Moulder JF, Stickle WF, Sobol PE. Handbook of X-ray photoelectron spectroscopy. *Phys Electron* 1995;1(1):10.
- [19] Han Z, Zhang J, Yu Y, Cao W. A new anode material of silver photo-deposition on TiO₂ in DSSC (c). *Mater Lett* 2012;70:193–6.
- [20] Atwater HA, Polman A. Plasmonics for improved photovoltaic devices. *Nat Mater* 2010;9(3):205–13.
- [21] Amiri O, Salavati-Niasari M, Farangi M, Mazaheri M, Bagheri S. Stable plasmonic-improved dye sensitized solar cells by silver nanoparticles between titanium dioxide layers. *Electrochim Acta* 2015;152:101–7.
- [22] Lim SP, Pandikumar A, Lim HN, Ramaraj R, Huang NM. Boosting photovoltaic performance of dye-sensitized solar cells using silver nanoparticle-decorated N,S-Co-doped-TiO₂ photoanode. *Sci Rep* 2015;5:11922.
- [23] Lim SP, Pandikumar A, Huang NM, Lim HN. Silver/titania nanocomposite-modified photoelectrodes for photoelectrocatalytic methanol oxidation. *Int J Hydrogen Energy* 2014;39(27):14720–9.
- [24] Catchpole KR, Polman A. Plasmonic solar cells. *Opt Express* 2008;16(26):21793.
- [25] Gong J, Liang J, Sumathy K. Review on dye-sensitized solar cells (DSSCs): Fundamental concepts and novel materials. *Renew Sustain Energy Rev* 2012;16(8):5848–60.
- [26] Lim SP, Pandikumar A, Huang NM, Lim HN. *RSC Adv* 2014;4(i):38111–8.
- [27] Zhao G, Kozuka H, Yoko T. Effects of the incorporation of silver and gold nanoparticles on the photoanodic properties of rose bengal sensitized TiO₂ film electrodes prepared by sol-gel method. *Sol Energy Mater Sol Cells* 1997;46(3):219.
- [28] Kim JBBSG, Ju MJ, Choi IT, Choi WS, Choi H-J, Kim HK. Nb-doped TiO₂ nanoparticles for organic dye-sensitized solar cells. *RSC Adv* 2013;3:16380–6.
- [29] Yusoff MM, Archana RJPS, Gupta A. Tungsten doped titanium dioxide nanowires for high efficiency dye-sensitized solar cells. *Phys Chem Chem Phys* 2014;16:7448–54.
- [30] Hagfeldt A, Nissfolk GBJ, Fredin K. Recombination and transport processes in dye-sensitized solar cells investigated under working conditions. *J Phys Chem* 2006;110:17715–8.